

# Theoretical Assessment of Norfloxacin Redox and Photochemistry

Klefah A. K. Musa<sup>†</sup> and Leif A. Eriksson<sup>\*,†,‡</sup>

Örebro Life Science Center, School of Science and Technology, Örebro University, 701 82 Örebro, Sweden, and School of Chemistry, National University of Ireland, Galway, Ireland

Received: May 19, 2009; Revised Manuscript Received: August 6, 2009

Norfloxacin, 1-ethyl-6-fluoro-1,4-dihydro-4-oxo-7-(1-piperazinyl)-3-quinolinecarboxylic acid, NOR, is an antibiotic drug from the fluoroquinolone family. The different protonation states of this drug formed throughout the pH range is studied by means of density functional theory (DFT) and the spectra of the NOR species computed using time-dependent DFT. Details about their photochemistry are obtained from investigating the highest occupied and lowest unoccupied molecular orbitals. The predominant species under physiological pH, the zwitterion, is the most photoliable one, capable of producing singlet oxygen or/and superoxide radical anions from its triplet state. In addition, the main photodegradation step, defluorination, occurs more easily from this species compared with the other forms. The defluorination from the excited triplet state requires passing a barrier of 16.3 kcal/mol in the case of the zwitterion. The neutral and cationic forms display higher transition barriers, whereas the reaction path of defluorination is completely endothermic for the anionic species. The theoretical results obtained herein are in line with previous experimental data.

## 1. Introduction

Fluoroquinolones (FQs) constitute a relatively new class of antibiotics that was introduced to clinical therapy in the 1980s. They display a broad spectrum of antibacterial activity including strong effects on Gram-negative aerobic and anaerobic organisms as well as Gram-positive and atypical pathogens. FQs belong to a second generation of antibiotic drugs used mainly to treat bacterial urinary tract infections, sexually transmitted diseases, prostatitis, selected pneumonias, and skin infections.<sup>1–3</sup> They produce their pharmacological action by enzymatic inhibition, where the primary target is the bacterial enzyme DNA gyrase or topoisomerase II, an enzyme involved in DNA replication and repair.<sup>4–6</sup>

FQs exhibit, although at low frequency, side effects in the gastrointestinal tract (GIT) and central nervous system and are known to induce severe photosensitivity. Unfortunately, the cause of the abnormal photosensitivity of the FQs, and its relationship to chemical structures, is still not clear.<sup>7</sup>

Phototoxicity is an important event that introduces serious limitations to drug usage. Drug-induced phototoxic reactions are elicited by absorption of photoenergy by drugs distributed in the skin, which provokes a series of chemical reactions in the body. Since phototoxicity is one of the main side effects with many drugs, further theoretical and experimental studies are needed in order to shed light on explicit mechanisms and thus also help in developing possible routes to avoid these complications.

In general, FQs are very efficient photosensitizers; some of them are responsible for severe cutaneous reactions, while others seem to be potential photomutagenic and photocarcinogenic agents.<sup>8</sup> Several studies have shown that the degree of ionization significantly influences the photophysical and photochemical properties of FQs,<sup>1,9</sup> which ultimately can effect the reactions responsible for phototoxicity. In this context, FQs have been

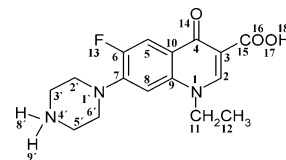


Figure 1. Chemical structure of  $N_4$ -protonated NOR.

attributed to the generation of several reactive oxygen species.<sup>10–15</sup> UVA-irradiated samples containing FQs have been shown to generate hydrogen peroxide. Hydroxide radical formation has been indicated by the bleaching of P-nitrosodimethylaniline, and the reduction of cytochrome C in FQ containing samples irradiated with UV light is evidence of superoxide generation.<sup>11</sup> Singlet oxygen formation is equally important in FQ phototoxicity.<sup>1</sup> Interestingly, several quinolones have in vitro the capability to act as a peroxide to unsaturated lipid squalene in ethanol solution. This suggests that a nonsinglet oxygen mechanism is operative in addition to the singlet oxygen one.<sup>16</sup> In addition, defluorination is another pathway in the phototoxic mechanism of most FQs. This leads to formation of a highly reactive carbene at the site of defluorination<sup>17</sup> and provides a plausible mechanism for the phototoxic and photocarcinogenic properties of the parent compound.<sup>18</sup>

Norfloxacin, 1-ethyl-6-fluoro-1,4-dihydro-4-oxo-7-(1-piperazinyl)-3-quinolinecarboxylic acid, NOR, Figure 1, is a hydrophobic broad spectrum antibacterial drug belonging to the FQ family with a half-life of 3.0–4.5 h.<sup>19</sup> This drug was synthesized in 1980 by introducing a piperazine ring at carbon atom number 7 of quinolone;<sup>20,21</sup> due to the presence of the piperazinyl ring it shows a higher and broader range of antibacterial activity compared with other drugs in the same family lacking this ring.<sup>22</sup> The presence of a fluorine atom at position 6 provides an increase in the potency against Gram-negative organisms.<sup>23</sup> NOR is used in treatment of various bacterial diseases in humans<sup>24</sup> and in animals, such as the treatment of enteritis in dogs<sup>25</sup> and chronic respiratory disease in chickens.<sup>26</sup> NOR metabolism via N acetylation, oxidation, and breakdown of the piperazine ring has been studied in humans<sup>27</sup> and fungi.<sup>28</sup>

\* Corresponding author, leif.eriksson@nuigalway.ie.

<sup>†</sup> Örebro University.

<sup>‡</sup> National University of Ireland, Galway.

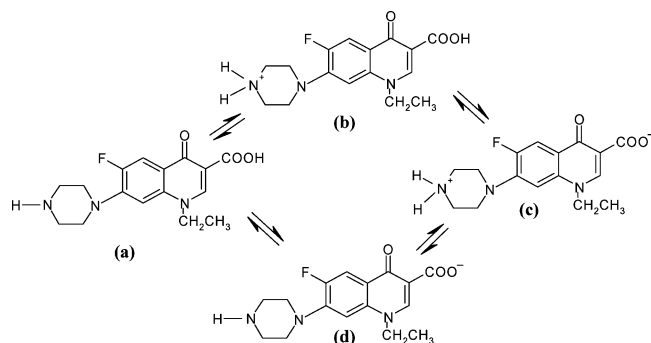


**Figure 2.** The different protonation states of norfloxacin depending on pH: (a) neutral, (b) cation, (c) zwitterion, and (d) anion.

Most of the FQ molecules have two proton binding sites, the 4'-nitrogen of the piperazinyl ring and the quinolone carboxylic group, and hence also two main protolytic equilibria, with  $pK_a$  at approximately 8.5 and 5.5–6.5, respectively. Hence the NOR compound will exist in different forms depending on the pH.<sup>29</sup> At neutral or physiological pH, NOR is present predominantly as a zwitterion (in which the carboxylic group is deprotonated and the peripheral piperazine nitrogen atom is protonated). This is the most photolabile form, with  $pK_a$  values of 6.2 and 8.5.<sup>30</sup> At pH 10 more than 90% will be in the anionic form, whereas protonation of the carboxylic group occurs when the pH is decreased to 4.5 thus forming the cationic species.<sup>31,32</sup> The pH and the presence of salts are determining factors in NOR photodegradation.<sup>32,33</sup> The different species are displayed in Figure 2.

The NOR UV-absorption spectrum in phosphate buffer at pH 7.4 is characterized by an intense absorption band which peaks in the UVB region at 260–280 nm and a weaker band in the UVA region at 320–340 nm with a long tail extending up to 380 nm. Other intense bands are also present at wavelengths less than 250 nm.<sup>29</sup>

NOR has been reported to cause photosensitivity in animals and humans,<sup>1</sup> where the photodegradation of NOR is mediated by excitation and intersystem crossing to the lowest triplet state.<sup>29</sup> The photolabile species of NOR (zwitterion) also has ability to release fluoride via the triplet state. This takes place through either ionic or radical pathways, depending on the type of solvent used.<sup>29,33</sup> Although this is an uncommon reaction for fluoroaromatics in general, due to the strength of the carbon–fluorine bond (dissociation energy  $\sim 120$  kcal/mol),<sup>34,36</sup> the heterolytic C–F bond cleavage is more efficient for the zwitterion (giving a cation) than for the cationic species (giving a dication) or the anionic form (giving an unstable zwitterion).<sup>32</sup> The reaction will not be homolytic because of the energy of this bond is larger than that of the energy of the excited singlet state.<sup>33</sup>

NOR phototoxicity related to DNA damage caused by reactive oxygen species primarily involves singlet oxygen which is produced with a maximum around pH 8–9 because of weaker self-quenching of singlet oxygen in this pH range.<sup>1</sup> The lowest excited singlet state of NOR is however not sufficiently reactive, and the important reaction channel is through intersystem crossing (ISC) to the triplet state. The lowest triplet state will cause C–F bond cleavage through a solvent-mediated process and proceeds via a cyclohexadienyl anionic adduct. A defluorination mechanism induced by electron transfer from inorganic anions to the NOR triplet state is found in the presence sulfite or phosphate buffer,<sup>29</sup> and the photoproducts change according to medium used.

Irradiation in neat water or in the presence of  $5 \times 10^{-4}$  M sodium hydrogen carbonate at pH 7.2 will lead to the formation of the corresponding phenols by nucleophilic substitution of fluorine in position 6 by a hydroxyl group. No phenols were however found in neutral sulfite buffer, and only reductive defluorination was observed.<sup>37</sup> The photoinduced formation of the 6-OH derivative is proposed to occur through one of two mechanisms: either by heterolytic cleavage of the C–F bond thereby forming an aryl cation or by water addition followed by loss of (hydrogen) fluoride.<sup>37</sup> Evidence about which mechanism constitutes the main pathway is still lacking, but it is well established that the process occurs through the excited triplet state of monofluorinated FQs. This is supported by the fact that the reaction is inhibited by the presence of water-soluble naphthalene derivatives such as naproxen, which acts as triplet quencher.<sup>38</sup>

As mentioned above, pH also plays an important role in the photodegradation pathways of these types of compounds. Intramolecular electron transfer can occur from the deprotonated piperazine ring to the quinolone system at high pH, providing an efficient energy-dissipating channel causing deactivation of the singlet excited state. Because of this, neither fluorescence emission nor topical transient (T-T) absorption can be detected in basic media. The 4'-N-acetyl derivative of NOR is used in order to surpass the deactivation pathway in alkaline medium, due to the lower availability of the 4'-N lone pair of the piperazinyl ring.<sup>38</sup>

Bicarbonate and phosphate buffer solutions furthermore enhance the transformation of the primary triplet state into a second transient species. The mechanism of formation and the nature of this species are not clear as yet, but it is suggested to also be a triplet state. It is characterized by shorter lifetime than the primary triplet and absorbs at longer wavelength. In phosphate buffer, the formation of the secondary (radical anion) species was suggested to occur due to electron transfer from the phosphate dianion to the primary triplet state. In addition, the proposed secondary triplet of some FQs including NOR was not quenched by naphthalene derivatives as opposed to the primary triplet states, indicating that the energy of the former is lower than that of the latter. Interestingly, once the medium is a weak base such as acetate or oxalate, the above results are not observed. This suggests a base-catalyzed deprotonation process in the FQ triplet state and is considered an unusual process as no triplet is formed by direct excitation from the anionic ground state.<sup>39</sup>

## 2. Computational Methodology

All geometries of NOR in its different protonation states, as well as the radical anion and cation were optimized in both singlet and triplet states at the hybrid Hatree–Fock Density Functional Theory B3LYP/6-31G(d,p) level. Solvent effects were taken into consideration implicitly, through single point calculations on the optimized geometries at the same level of theory, including the integral equation formulation of the polarized continuum model (IEFPCM).<sup>40–42</sup> Water was used as solvent, through the value 78.39 for the dielectric constant in the IEFPCM calculations. Frequency calculations were performed on the optimized geometries at the same level of theory, to ensure the systems to be local minima (no imaginary vibration frequencies) and to extract zero-point vibrational energies (ZPE) and thermal corrections to the Gibbs free energies at 298 K. Excitation spectra of the neutral, anion, cation, and zwitterion species were calculated using the time-dependent formalism (TD-DFT<sup>43–45</sup>), at the same level of theory. In the current study,

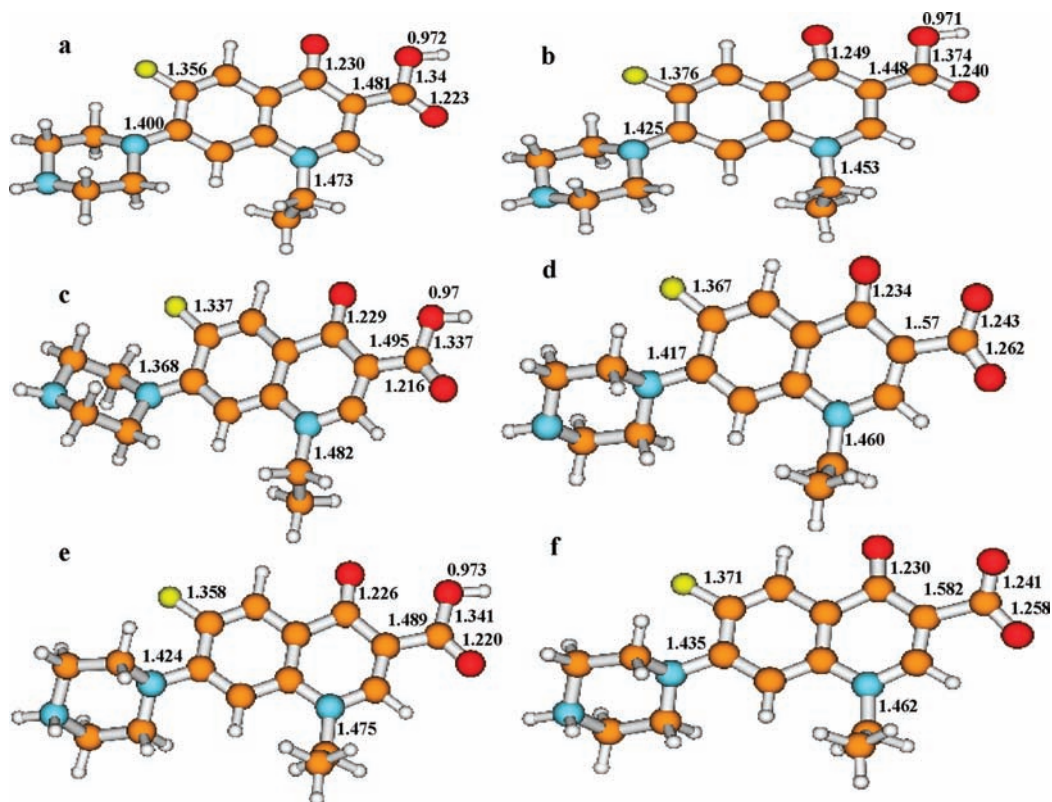


**Figure 3.** B3LYP/6-31G(d,p) optimized structures of NOR: (a) neutral ground state, (b) radical anion, (c) radical cation, (d) deprotonated (anion), (e) protonated (cation), (f) zwitterion.

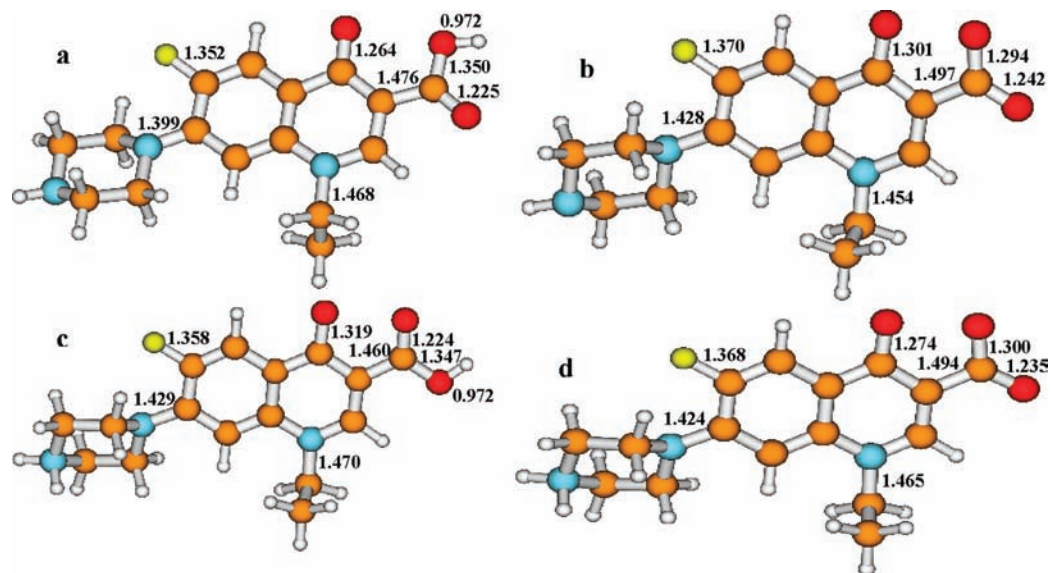


**Figure 4.** B3LYP/6-31G(d,p) optimized structures of the triplet states of NOR: (a) neutral form, (b) deprotonated (anion), (c) protonated (cation), (d) zwitterion.

only vertical singlet excitations are considered in this respect, albeit recent methodological improvements have been proposed to enable the study of adiabatic excitations and vibronic effects, respectively.<sup>46,47</sup> The numbering scheme of the atoms used throughout the study is given in Figure 1. All calculations were performed with the Gaussian 03 program package.<sup>48</sup>

### 3. Results and Discussion

**3.1. Optimized Structures.** The optimized structures of the different species are displayed in Figures 3 (singlet ground

states) and 4 (first excited triplet states). Overall, there are very small changes in bond lengths of the optimized structures in the singlet ground states. The C<sub>7</sub>–N<sub>1</sub> bond length is increased (decreased) by 0.03 (0.13) Å in the radical anion (radical cation), respectively, compared to the neutral parent compound. The changes are even smaller between the different protonated species. The C<sub>6</sub>–F<sub>13</sub> bond length lies within the range 1.356–1.376 Å for all species studied. The main change in optimized structures is instead found in the dihedral angle (C<sub>6</sub>–C<sub>7</sub>–N<sub>1</sub>–C<sub>2</sub>) which connects the piperazinyl and quinolone

**TABLE 1: B3LYP/6-31G(d,p) ZPE-Corrected Electronic Energies in Gas Phase, and IEFPCM-B3LYP/6-31G(d,p) Gibbs Free Energies in Aqueous Solution<sup>a</sup>**

system <sup>b</sup>	$E_{(ZPE)}$	$\Delta E_{(ZPE)}$	$\Delta G_{aq}^{298}$	$\Delta \Delta G_{aq}^{298}$	$\mu_{aq}$
Singlet Ground States					
N <sup>singlet</sup>	-1110.014484	0	-1110.099536	0	10.95
A <sup>singlet</sup>	-1109.448515	355.15	-1109.624401	298.15	32.18
C <sup>singlet</sup>	-1110.372557	-224.69	-1110.556589	-286.81	32.99
Z <sup>singlet</sup>	-1109.873857	88.24	-1110.079636	12.49	55.93
Radical Anion and Radical Cation for the Neutral Form					
N <sup>•-</sup> (EA)	-1110.016468	-1.25	-1110.171553	-45.19	18.68
N <sup>•+</sup> (IP)	-1109.759068	160.28	-1109.910626	118.54	18.54
Triplet States					
N <sup>triplet</sup>	-1109.910039	65.54	-1109.995906	65.03	12.50
A <sup>triplet</sup>	-1109.381862	396.98	-1109.531416	356.5	23.76
C <sup>triplet</sup>	-1110.274506	-163.17	-1110.445689	-217.22	27.36
Z <sup>triplet</sup>	-1109.834935	112.67	-1109.990033	68.71	47.29
Singlet-Triplet Gaps for Each Species					
N <sup>singlet</sup>	-1110.014484	0	-1110.099536	0	10.95
N <sup>triplet</sup>	-1109.910039	65.54	-1109.995906	65.03	12.50
A <sup>singlet</sup>	-1109.448515	0	-1109.624401	0	32.18
A <sup>triplet</sup>	-1109.381862	41.83	-1109.531416	58.35	23.76
C <sup>singlet</sup>	-1110.372557	0	-1110.556589	0	32.99
C <sup>triplet</sup>	-1110.274506	61.53	-1110.445689	69.59	27.36
Z <sup>singlet</sup>	-1109.873857	0	-1110.079636	0	55.93
Z <sup>triplet</sup>	-1109.834935	24.42	-1109.990033	56.23	47.29

<sup>a</sup> Absolute energies in a.u., relative energies in kcal/mol. Dipole moments  $\mu$  (debye) in aqueous solution. <sup>b</sup> Labels N, A, C, and Z refer to the different protonation states; see Figure 2.

rings. The values of the dihedral angles are 56, 60, 28, -60, -61, and -63° for the neutral, radical anion, radical cation, anion, cation, and zwitterion moieties, respectively. In addition, the optimized structures of the triplet states of the NOR species display no major changes compared with the singlet ground state parent molecules. For example, the carbonyl bond of the quinolone ring (C<sub>4</sub>-O<sub>14</sub>) is elongated by only 0.03, 0.07, 0.09, and 0.04 Å for the neutral, anion, cation, and zwitterion, respectively, and the dihedral angle mentioned above is in the optimized triplet states of the neutral, anion, cation, and zwitterion only modified a few degrees.

One of the key parameters in the photodegradation of other carboxylic compounds of medical interest such as nonsteroidal anti-inflammatory drugs (NSAIDs) is the C-C bond connecting to the carboxylic group (C<sub>3</sub>-C<sub>15</sub> in NOR). In, e.g., ketoprofen, this bond is elongated significantly upon deprotonation, and spontaneously dissociates in the excited triplet. For the NOR compound, however, no such trends are seen, indicating that decarboxylation is most likely not a key reaction in the phototoxicity of norfloxacin.

**3.2. Energetics of NOR Species.** In Table 1 we display the calculated absolute and relative ZPE corrected electronic energies and Gibbs free energies in aqueous solution at 298 K, as well as the dipole moments in aqueous solution for the different NOR species. The results show that the zwitterion lies about 88 kcal/mol above the neutral parent molecule in the gas phase, which is reduced by more than 75 kcal/mol (to 12.5 kcal/mol) when bulk solvation is taken into consideration. The fact that the neutral species remains the most stable can be due to the geometries being optimized in vacuo, insufficient polarization of the PCM model employed, or explicit hydrogen bonding interaction not present in the calculations. Including the chemical potential of a free proton in aqueous solution at 298 K, -268.68 kcal/mol,<sup>49</sup> we also note that at neutral pH, the protonated species will be formed spontaneously, whereas the anion will not. The energy difference between the neutral form and the

radical anion, the electron affinity (EA), is calculated to be only 1.2 kcal/mol (0.054 eV) in gas phase but 45.2 kcal/mol (1.96 eV) in the solvent phase. The ionization potential (IP) is in the gas phase 160.3 kcal/mol (6.95 eV) and 118.5 kcal/mol (5.14 eV) including bulk solvation. The charge stabilization by the polar environment is hence significant in these systems.

The dipole moments of these species change dramatically with protonation state. The neutral form is roughly 11 D and increases to about 32 D for the anionic and cationic forms of NOR. The dipole moment is increased further for the zwitterion, and reaches 56 D. The radical anion and radical cation have similar dipole moments, around 18 D. This fluctuation in dipole moments between different states and species was also observed in experimental studies.<sup>13,50</sup> The very high dipole moments are explained by investigating the charge redistribution between the subunits of these molecules; Table 2 (discussed more below).

Once the NOR molecule has absorbed UV light at the appropriate wavelength, it will reach the singlet excited state, which is relatively unreactive. An important decay channel is the intersystem crossing (ISC) from S<sub>1</sub> giving the excited triplet state, as the 4-quinolone moiety is an efficient singlet-triplet converter.<sup>51</sup> From previous experimental data, the quantum yield for triplet state formation is known to be dependent on the molar triplet absorption coefficient. For the molecular species in phosphate buffer solution at pH 7-7.4, the triplet quantum yield has been measured to be  $\geq 0.5$ , with a lifetime of 3.5  $\mu$ s.<sup>29,51,52</sup> The calculated singlet-triplet gaps for the neutral, anion, cation, and zwitterion are 65, 58.4, 69.6, and 56.2 kcal/mol, respectively, in the solvent phase. This is in good agreement with laser flash photolysis experiments giving an absolute value of the triplet energy of NOR in the range between 260 and 280 kJ/mol (62.1-66.9 kcal/mol).<sup>51,52</sup> The relation between the ground states and the excited triplet states of the different protonation forms is given in Figure 5.

**TABLE 2: Mulliken Atomic Charges (B3LYP/6-31G(d,p) level) for Selected Atoms of NOR and Its Three Subunits COO(H), QN, and PP<sup>a</sup>**

system	C <sub>4</sub>	C <sub>6</sub>	C <sub>9</sub>	C <sub>12</sub>	C <sub>15</sub>	F <sub>13</sub>	N <sub>1'</sub>	N <sub>4'</sub>	N <sub>1</sub>	O <sub>14</sub>	O <sub>16</sub>	O <sub>17</sub>	H <sub>18</sub>	COO(H)	QN	PP
N <sup>singlet</sup>	0.393	0.334		-0.319	0.560	-0.295	-0.523	-0.504	-0.554	-0.512	-0.514	-0.466	0.317	-0.104	0.248	-0.144
N <sup>*-</sup>	0.350		0.302	-0.309	0.508	-0.335	-0.520	-0.505	-0.540	-0.594	-0.588	-0.502		-0.308	-0.438	-0.254
N <sup>*+</sup>	0.414	0.369	0.369	-0.325	0.588	-0.252	-0.462	-0.492	-0.569	-0.441	-0.474	-0.461		-0.005	0.755	0.250
N <sup>triplet</sup>	0.341	0.330	0.328	-0.319	0.556	-0.287	-0.523	-0.503	-0.513	-0.467	-0.497	-0.472	0.316	-0.098	0.234	-0.136
A <sup>singlet</sup>	0.359	0.312	0.304	-0.315	0.530	-0.319	-0.521	-0.504	-0.551	-0.525	-0.644	-0.586		-0.699	-0.086	-0.215
A <sup>triplet</sup>	0.297	0.312	0.309	-0.311	0.557	-0.329	-0.515	-0.505	-0.562	-0.495	-0.433	-0.580		-0.456	-0.285	-0.259
C <sup>singlet</sup>	0.405	0.336	0.322	-0.321	0.574	-0.299	-0.514	-0.492	-0.563	-0.489	-0.494	-0.462	0.330	-0.052	0.335	0.717
C <sup>triplet</sup>	0.307	0.342	0.323	-0.319	0.591	-0.304	-0.506	-0.490	-0.568	-0.338	-0.501	-0.420	0.346	0.016	0.300	0.684
Z <sup>singlet</sup>	0.373	0.311	0.320	-0.316	0.544	-0.323	-0.510	-0.490	-0.554	-0.505	-0.627	-0.571		-0.654	-0.000	0.654
Z <sup>triplet</sup>	0.348	0.330	0.327	-0.316	0.585	-0.322	-0.498	-0.395	-0.561	-0.480	-0.538	-0.372		-0.325	-0.048	0.373

For C<sup>singlet</sup>: H<sub>g</sub> = 0.345, H<sub>y</sub> = 0.360. C<sup>triplet</sup>: H<sub>g</sub> = 0.340, H<sub>y</sub> = 0.356. For Z<sup>singlet</sup>: H<sub>g</sub> = 0.348, H<sub>y</sub> = 0.338. Z<sup>triplet</sup>: H<sub>g</sub> = 0.209, H<sub>y</sub> = 0.229

<sup>a</sup> COO(H) is the carboxylic group at position 3 of quinolone ring (QN), and PP is the piperazinyl ring. For atomic labeling, see Figure 1.

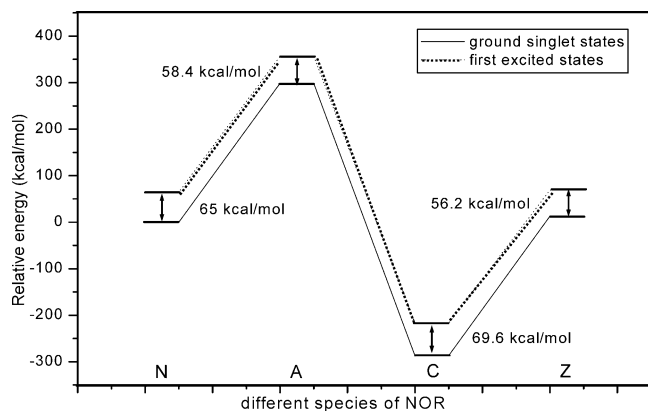


**Figure 5.** Energies of the ground singlet states and the corresponding first excited triplet states of the four protonation forms neutral (N), anion (A), cation (C), and zwitterion (Z). The ground state of the neutral species is set to zero.

In the presence of molecular oxygen, the NOR triplet state will quench by one of the following processes



The first reaction is energetically feasible as the excitation energy of ground state molecular oxygen leading to the formation of singlet oxygen is 22.5 kcal/mol.<sup>54</sup> This will hence lead to the generation of highly reactive and cytotoxic singlet oxygen species. The singlet oxygen quantum yield for this process has experimentally been measured to be 0.08, with the highest quantum yield observed at pH 7–8, whereas the production is reduced at lower or higher pH.<sup>17,51</sup> The second reaction involves the photogeneration of superoxide and a NOR radical cation, which, since the adiabatic electron affinity of molecular oxygen to generate superoxide in solution is estimated to 90.2 kcal/mol (3.91 eV),<sup>55</sup> is exergonic by approximately 36 kcal/mol. The quantum yield for superoxide production is experimentally determined to be 0.25.<sup>17</sup> The generated reactive oxygen species will effect the oxidant–antioxidant balance of the biological system leading to different harmful effects like lipid peroxidation, hemolysis of erythrocytes and neutrophils, and DNA perturbation (photogenotoxicity). In addition, the binding between NOR and DNA has been studied experimen-

tally and shows that induction of a structural alteration and perturbation in DNA precede DNA cleavage.<sup>53</sup> The third reaction, finally, is a simple physical quenching.

The NOR molecule has an electron donor, the piperazinyl group, and an electron acceptor, the carboxylic group, and is considered a good twisted charge transfer molecule in the excited state. Experimental data show that the intramolecular charge transfer is accelerated in water (zwitterionic form) compared with methanol (neutral form)<sup>22,50</sup> which is in agreement with the current data. Except for the neutral form, charge transfer occurs in all species once the molecule is excited and the triplet state is formed, as seen in Table 2. For the deprotonated form negative partial charge is transferred from the carboxylic moiety and redistributed on the quinolone and piperazinyl rings. The same effect is seen in the formation of the triplet state of the protonated cationic form. The zwitterion has most of its charge distributed between the carboxylic and piperazinyl subunits in the singlet ground state. In the triplet state, this balance is maintained, but with much smaller values of the charges. The unpaired spin density (Table 3) of the radical anion is found mainly on the quinolone ring, while in the radical cation, it is distributed almost equally between the quinolone and piperazinyl rings. For the triplet state of the neutral form, the spin density is mainly on the quinolone ring, similar to the protonated species. In the anion on the other hand, the spin is mainly located on quinolone ring and about 0.5 electrons on the carboxylic moiety. This is similar to the zwitterion triplet state, although we also see some unpaired spin on the piperazinyl ring in this case.

### 3.3. Orbital Configuration and Spectra of NOR Species.

The difference in photochemistry between the four NOR species can be further rationalized by inspection of their molecular orbitals, displayed in Figure 6. For the neutral form, the highest occupied molecular orbital (HOMO) and HOMO-1 are localized on the quinolone ring and to less extent to N<sub>1'</sub> of the piperazinyl ring, whereas HOMO-2 is localized mainly on the carbonyl group of the quinolone ring. LUMO and LUMO+2 are localized on the quinolone ring only, whereas the LUMO+1 orbital has minor components also on the N<sub>1'</sub> atom of the piperazinyl ring and on the carboxylic moiety. The HOMO, HOMO-1, and HOMO-2 orbitals of the anion and the zwitterion are very similar and localized on the carboxylic moieties, whereas their LUMOs are completely different. The LUMO orbitals of the anion form and LUMO+2 of the zwitterion are localized on the quinolone ring, whereas LUMO and LUMO+1 of the zwitterion are localized on the peripheral amino group (N<sub>4'</sub>) of the piperazinyl ring. The HOMO, HOMO-1, and HOMO-2 of the cation finally are localized on the quinolone ring, the

**TABLE 3: Atomic Spin Densities (B3LYP/6-31G(d,p) Level) on Selected Atoms and Groups for the Radical Species of NOR<sup>a</sup>**

system	C <sub>2</sub>	C <sub>3</sub>	C <sub>4</sub>	C <sub>5</sub>	C <sub>6</sub>	C <sub>7</sub>	C <sub>8</sub>	C <sub>10</sub>	N <sub>1'</sub>	N <sub>1</sub>	O <sub>14</sub>	O <sub>17</sub>	H <sub>8'</sub>	H <sub>9'</sub>	COO(H)	QN	PP
N <sup>•-</sup>	0.609						0.149								0.080	0.918	0.002
N <sup>•+</sup>					0.231			0.306	0.357		0.173				-0.001	0.529	0.472
N <sup>triplet</sup>	0.581	0.298			0.210		0.137	0.153		0.282	0.447				0.058	1.931	0.011
A <sup>triplet</sup>	0.278		0.230	0.270							0.589	0.499			0.494	1.488	0.018
C <sup>triplet</sup>	0.169		0.298	0.265		0.233					0.892	0.147			0.150	1.831	0.019
Z <sup>triplet</sup>	0.111			0.217		0.187	0.118				0.435	0.614	0.125	0.136	0.619	1.063	0.318

<sup>a</sup> COO(H) is the carboxylic group at position 3 of the quinolone ring (QN) and PP is the piperazinyl ring. For atomic labeling, see Figure 1.

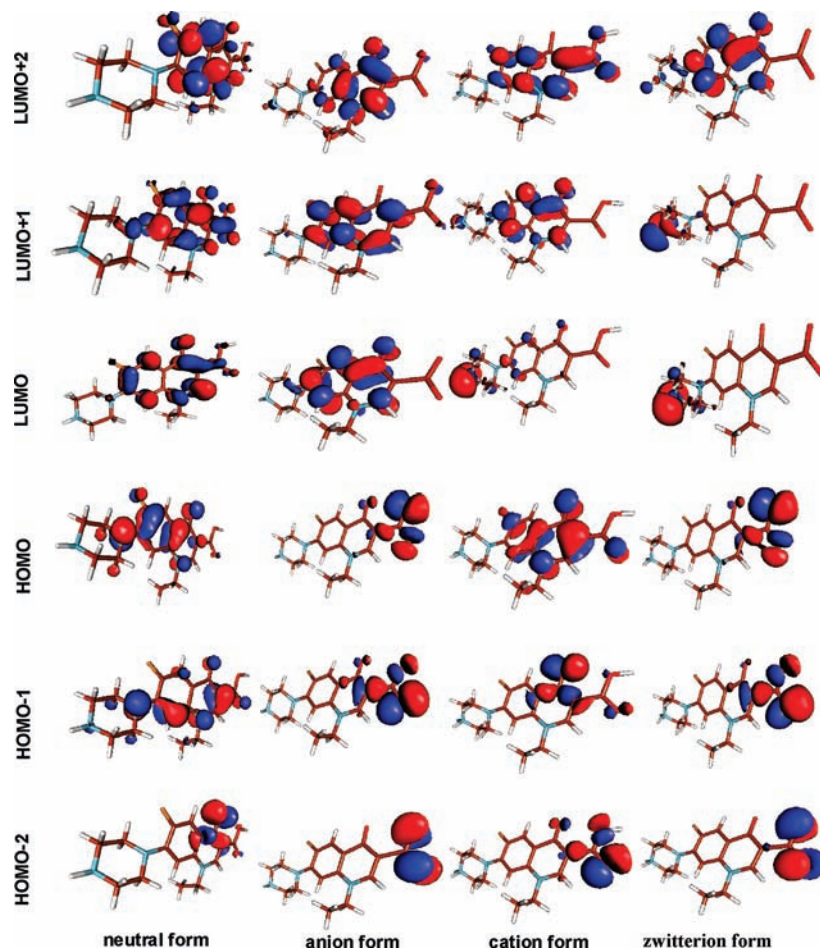


**Figure 6.** Ground-state orbitals of different protonation states of norfloxacin. Piperazinyl ring to the left and carboxylic group to the right of each molecule.

carbonyl group of the quinolone ring, and on the carboxylic moiety, respectively. For this species the LUMO is localized on the peripheral amino group of the piperazinyl ring, LUMO+1 on the quinolone ring, and LUMO+2 on the quinolone ring and the carboxylic moiety. On the basis of the orbital structures, we can hence assume the photochemical behavior resulting from HOMO  $\rightarrow$  LUMO excitation in, e.g., neutral NOR, to be very different from that of the zwitterion form. The former will be of  $\pi, \pi^*$  nature, whereas the latter is a charge transfer excitation. The orbital pictures are consistent with the charge redistribution and unpaired spin distributions of Tables 2 and 3.

The computed absorption spectra of the different species of NOR are shown in Figure 7. The main absorption peak of these species is located in the UVB region of the spectrum at 260–280 nm. The probability (oscillator strength) of absorption for the neutral form is higher than that for the anion and zwitterion in this region. All species also display weaker absorption in the 3–400 nm range, extending toward the visible region. These findings are in very good agreement with experimental data, as

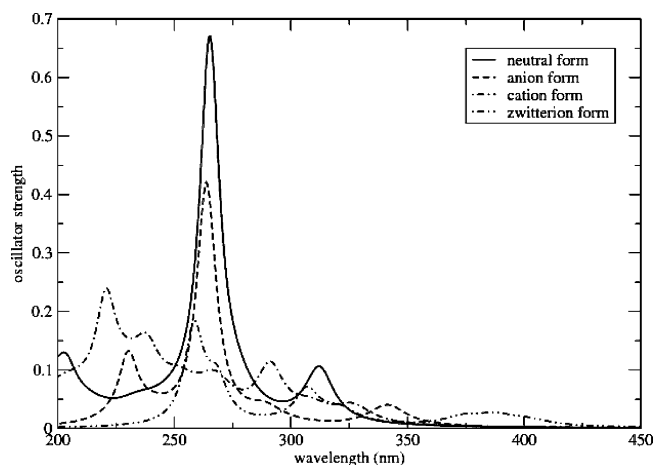


**Figure 7.** Computed UV spectra of the neutral (solid), anion (dashed), cation (dot-dashed), and zwitterion (double-dot-dashed) forms of NOR at the TD-B3LYP/6-31G(d,p) level.

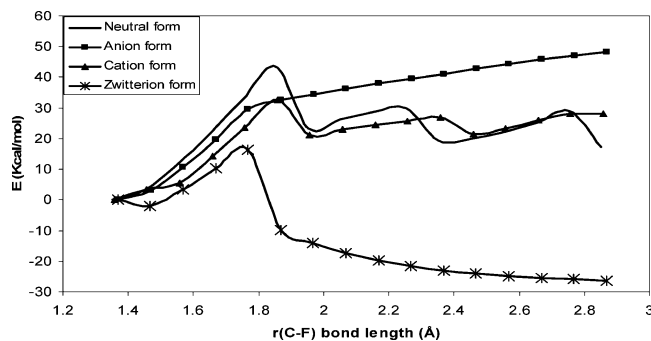


**Figure 8.** Scanned defluorination process for the neutral, anion, cation, and zwitterion of NOR.

mentioned in the introduction.<sup>29</sup> More bands are obtained at wavelength less than 250 nm, especially for the cationic, zwitterionic, and neutral forms, and this is also in good agreement with the experimental data.

**3.4. Defluorination.** As mentioned in the Introduction, the main photodegradation step for NOR is defluorination, a process that mainly occurs from the first excited triplet state. In Figure 8 we display the energy barrier for triplet defluorination, computed for each protonation state. The calculated barriers show that the zwitterion has an energy barrier of about 16.3 kcal/mol, with a C<sub>6</sub>–F<sub>16</sub> transition state distance at 1.77 Å. This is in line with experimental results which show that the zwitterion is the most photolabile form of the NOR species. The defluorination energy barrier of the protonated form is about double that estimated for the zwitterion (32.7 kcal/mol), with a TS distance of 1.85 Å. The energy barrier of this process for the neutral form lies higher than the first two species and is calculated to be 43.3 kcal/mol and with a TS distance similar to that obtained for the cation. The energy curve of the anion shows that the defluorination process in this case is endothermic. These results are in agreement with the previous experimental studies where the heterolytic C–F bond cleavage is more efficient from the zwitterion (resulting in a cation) than from the protonated species (giving a dication) or the deprotonated form (giving an unstable zwitterion).<sup>32</sup> Once defluorination has occurred, the cationic site at C<sub>6</sub> becomes activated. The product formed depends on the environmental conditions, whereby in neat water or in the presence of  $5 \times 10^{-4}$  M sodium hydrogen carbonate at pH 7.2 the corresponding phenols will form through addition of a water molecule at C<sub>6</sub> followed by deprotonation, whereas only reductive defluorination was observed in neutral sulfite buffer.<sup>37</sup> Flash photolysis investigations revealed that the reaction proceeds from the triplet state and involves a long-lived intermediate (3.6 μs). The quantum yield of this process is proportional to the electrophilicity of the heterocyclic ring which for NOR in aqueous medium is in the range 0.06–0.01.<sup>33</sup>

#### 4. Conclusions

Geometries, electronic distributions and photochemical behavior of the different protonation states of the antibiotic compound norfloxacin, a member of the fluoroquinolone family, have been studied by means of DFT/B3LYP/6-31G(d,p) methodology. The optimized structures of the neutral, deprotonated, protonated, and zwitterionic species show that very small changes in bond lengths occur when these molecules are optimized in their singlet or triplet states. Instead the main geometrical changes occur in the dihedral angle (C<sub>6</sub>–C<sub>7</sub>–N<sub>1</sub>–C<sub>2</sub>) which connects the piperazinyl and quinolone rings.

The computed spectra of the neutral, anion, cation, and zwitterionic forms show that the main absorbance peaks are

obtained at wavelengths in the UVB region of the spectrum (260–280 nm). The zwitterion also shows a weaker peak in the UVA region at 320–340 nm with a long tail extending up to 380 nm, in good agreement with experimental data.<sup>29</sup>

The electron affinity (EA) of the neutral form is calculated to be 1.25 kcal/mol (0.054 eV) in the gas phase, while in the solvent phase it is 45.2 kcal/mol (1.96 eV). The ionization potentials (IP) in the gas phase are 160.3 kcal/mol (6.95 eV) and 118.5 kcal/mol (5.14 eV) using bulk solvation. The calculated singlet–triplet gaps for the neutral, anion, cation, and zwitterion are 65, 58.4, 69.6, and 56.2 kcal/mol, respectively, in the bulk solvent. This is in good agreement with experimental results according to which the absolute value of the triplet energy for NOR, estimated by means of laser flash photolysis, is found to be in the range of 62.1–66.9 kcal/mol.<sup>51,52</sup>

The efficiency of the photodecomposition is related to the internal charge transfer character of the excited state which is explored by investigating Mulliken charge distributions and plotting molecular orbitals of the different NOR species. These data also support the observation that the predominant species under physiological pH, the zwitterion, is the most photolabile one. Energetically, it will be capable to generate reactive oxygen species such as singlet oxygen or/and superoxide radical anion. In addition, the main photodegradation step, defluorination, occurs more easily in this species compared to the other forms. Defluorination from the excited triplet state requires passing a transition barrier of 16.3 kcal/mol in the case of the zwitterion, which explains also the long lifetime of the triplet intermediate (3.6 μs).

The present work provides a theoretical overview of the energetics of the different NOR species and the charge transfer character between the subunits of the drug, of relevance when designing new antibiotics related to this family with less or no phototoxic side effects.

**Acknowledgment.** The MENA programme (K.A.K.M.), the Swedish Science Research Council, and the Faculty of Science and Technology at Örebro University (L.A.E.) are gratefully acknowledged for financial support. We also acknowledge generous grants of computing time at the National Supercomputing Center (NSC) in Linköping.

#### References and Notes

- (1) Bilski, P.; Martinez, L. J.; Koker, E. B.; Chignell, C. F. *Photochem. Photobiol.* **1996**, *64*, 496.
- (2) <http://ezinearticles.com/?Fluoroquinolone-Antibiotics-Classification,-Uses-and-Side-Effects&id=347625>.
- (3) Zhang, T.; Li, J. L.; Ma, X. C.; Xin, J.; Tu, Z. H. *Acta Pharmacol. Sinica* **2003**, *24*, 453.
- (4) Kassab, N. M.; Singh, A. K.; Kedor-Hackmam, E. R. M.; Santoro, M. I. R. *M. Rev. Bras. Cienc. Farm.* **2005**, *41*, 507.
- (5) El Bekay, R.; Alvarez, M.; Carballo, M.; Martin-Nieto, J.; Monteseirin, J.; Pintado, E.; Bedoya, F. J.; Sobrino, F. *J. Leukocyte Biol.* **2002**, *71*, 255.
- (6) Domagala, J. M.; Hanna, L. D.; Heifetz, C. L.; Hutt, M. P.; Mich, T. F.; Sanchez, J. P.; Solomon, M. *J. Med. Chem.* **1986**, *29*, 394.
- (7) Matsumoto, M.; Kojima, K.; Nagano, H.; Matsubara, S.; Yokota, T. *Antimicrob. Agents Chemother.* **1992**, *36*, 1715.
- (8) Mäkinen, M.; Forbes, P. D.; Stenback, F. J. *Photochem. Photobiol., B* **1997**, *37*, 182.
- (9) Sortino, S.; De Guidi, G.; Giuffrida, S.; Monti, S.; Velardita, A. *Photochem. Photobiol.* **1998**, *67*, 167.
- (10) Wagai, N.; Tawara, K. *Arch. Toxicol.* **1992**, *66*, 392.
- (11) Wagai, N.; Tawara, K. *Free Radical Res. Commun.* **1992**, *17*, 387.
- (12) Wagai, N.; Tawara, K. *Arch. Toxicol.* **1991**, *65*, 495.
- (13) Wagai, N.; Tawara, K. *Toxicol. Lett.* **1991**, *58*, 215.
- (14) Wagai, N.; Yamaguchi, F.; Sekiguchi, M.; Tawara, K. *Toxicol. Lett.* **1990**, *54*, 299.
- (15) Gonzalez, E.; Gonzalez, S. *J. Am. Acad. Dermatol.* **1996**, *35*, 871.

- (16) Fujita, H.; Matsuo, I. *Photodermatol., Photoimmunol. Photomed.* **1994**, *10*, 202.
- (17) Martinez, L. J.; Li, G.; Chignell, C. F. *Photochem. Photobiol.* **1997**, *65*, 599.
- (18) Martinez, L. J.; Sik, R. H.; Chignell, C. F. *Photochem. Photobiol.* **1998**, *67*, 399.
- (19) Rao, V.; Shyale, S. *Turk. J. Med. Sci.* **2004**, *34*, 239.
- (20) Koga, H.; Itoh, A.; Murayama, S.; Suzue, S.; Irikura, T. *J. Med. Chem.* **1980**, *23*, 1358.
- (21) SanzNebot, V.; Valls, I.; Barbero, D.; Barbosa, J. *Acta Chem. Scand.* **1997**, *51*, 896.
- (22) Park, H. R.; Oh, C. H.; Lee, H. C.; Lee, J. K.; Yang, K.; Bark, K. M. *Photochem. Photobiol.* **2002**, *75*, 237.
- (23) <http://dailymed.nlm.nih.gov/dailymed/drugInfo.cfm?id=3144>.
- (24) Lawrenson, R. A.; Logie, J. W. *J. Antimicrob. Chemother.* **2001**, *48*, 895.
- (25) Bhaumik, A. *Indian Vet. J.* **1997**, *74*, 246.
- (26) Sumano, L. H.; Ocampo, C. L.; Brumbaugh, G. W.; Lizarraga, R. E. *Br. Poult. Sci.* **1998**, *39*, 42.
- (27) Pauliukonis, L. T.; Musson, D. G.; Bayne, W. F. *J. Pharm. Sci.* **1984**, *73*, 99.
- (28) Parshikov, I. A.; Heinze, T. M.; Moody, J. D.; Freeman, J. P.; Williams, A. J.; Sutherland, J. B. *Appl. Microbiol. Biotechnol.* **2001**, *56*, 474.
- (29) Monti, S.; Sortino, S.; Fasani, E.; Albini, A. *Chem.—Eur. J.* **2001**, *7*, 2185.
- (30) Takacsnovak, K.; Noszal, B.; Hermecz, I.; Kereszturi, G.; Podanyi, B.; Szasz, G. *J. Pharm. Sci.* **1990**, *79*, 1023.
- (31) Sortino, S. *Photochem. Photobiol.* **2006**, *82*, 64.
- (32) Fasani, E.; Rampi, M.; Albini, A. *J. Chem. Soc., Perkin Trans. 2* **1999**, 1901.
- (33) Fasani, E.; Profumo, A.; Albini, A. *Photochem. Photobiol.* **1998**, *66*, 666.
- (34) Durand, A. P.; Brown, R. G.; Worrall, D.; Wilkinson, F. *J. Chem. Soc., Perkin Trans. 2* **1998**, 365.
- (35) Zhang, G. Z.; Wan, P. *J. Chem. Soc., Chem. Commun.* **1994**, 19.
- (36) Fagnoni, M.; Mella, M.; Albini, A. *Org. Lett.* **1999**, *1*, 1299.
- (37) Fasani, E.; Negra, F. F. B.; Mella, M.; Monti, S.; Albini, A. *J. Org. Chem.* **1999**, *64*, 5388.
- (38) Cuquerella, M. C.; Bosca, F.; Miranda, M. A. Photonucleophilic aromatic substitution of 6-fluoroquinolones in basic media: Triplet quenching by hydroxide anion. *J. Org. Chem.* **2004**, *69*, 7256.
- (39) Lorenzo, F.; Navaratnam, S.; Allen, N. S. Formation of secondary triplet species after excitation of fluoroquinolones in the presence of relatively strong bases. *J. Am. Chem. Soc.* **2008**, *130*, 12238.
- (40) Cances, E.; Mennucci, B.; Tomasi, J. *J. Chem. Phys.* **1997**, *107*, 3032.
- (41) Mennucci, B.; Tomasi, J. *J. Chem. Phys.* **1997**, *106*, 5151.
- (42) Cossi, M.; Scalmani, G.; Rega, N.; Barone, V. *J. Chem. Phys.* **2002**, *117*, 43.
- (43) Casida, M. E., Time-dependent density functional response theory for molecules. In *Recent advances in density functional methods, Part 1*; Chong, D. P., Ed.; World Scientific: Singapore, 1995; pp 155–192.
- (44) Stratmann, R. E.; Scuseria, G. E.; Frisch, M. J. *J. Chem. Phys.* **1998**, *109*, 8218.
- (45) Casida, M. E.; Jamorski, C.; Casida, K. C.; Salahub, D. R. *J. Chem. Phys.* **1998**, *108*, 4439.
- (46) Scalmani, G.; Frisch, M. J.; Mennucci, B.; Tomasi, J.; Cammi, R.; Barone, V. *J. Chem. Phys.* **2006**, *124*, 15.
- (47) Santoro, F.; Lami, A.; Improta, R.; Bloino, J.; Barone, V. *J. Chem. Phys.* **2008**, *128*, 17.
- (48) Frisch, M. J.; Trucks, G. W.; Schlegel, H. B.; Scuseria, G. E.; Robb, M. A.; Cheeseman, J. R.; Montgomery J. A., Jr.; Vreven, T.; Kudin, K. N.; Burant, J. C.; Millam, J. M.; Iyengar, S. S.; Tomasi, J.; Barone, V.; Mennucci, B.; Cossi, M.; Scalmani, G.; Rega, N.; Petersson, G. A.; Nakatsuji, H.; Hada, M.; Ehara, M.; Toyota, K.; Fukuda, R.; Hasegawa, J.; Ishida, M.; Nakajima, T.; Honda, Y.; Kitao, O.; Nakai, H.; Klene, M.; Li, X.; Knox, J. E.; Hratchian, H. P.; Cross, J. B.; Bakken, V.; Adamo, C.; Jaramillo, J.; Gomperts, R.; Stratmann, R. E.; Yazyev, O.; Austin, A. J.; Cammi, R.; Pomelli, C.; Ochterski, J. W.; Ayala, P. Y.; Morokuma, K.; Voth, G. A.; Salvador, P.; Dannenberg, J. J.; Zakrzewski, V. G.; Dapprich, S.; Daniels, A. D.; Strain, M. C.; Farkas, O.; Malick, D. K.; Rabuck, A. D.; Raghavachari, K.; Foresman, J. B.; Ortiz, J. V.; Cui, Q.; Baboul, A. G.; Clifford, S.; Cioslowski, J.; Stefanov, B. B.; Liu, G.; Liashenko, A.; Piskorz, P.; Komaromi, I.; Martin, R. L.; Fox, D. J.; Keith, T.; Al-Laham, M. A.; Peng, C. Y.; Nanayakkara, A.; Challacombe, M.; Gill, P. M. W.; Johnson, B.; Chen, W.; Wong, M. W.; Gonzalez, C.; Pople, J. A. *Gaussian 03, Revision B.02*; Gaussian, Inc.: Wallingford, CT, 2004.
- (49) Llano, J.; Eriksson, L. A. *J. Chem. Phys.* **2002**, *117*, 10193.
- (50) Park, H. R.; Seo, J. J.; Shin, S. C.; Lee, H. S.; Bark, K. M. *Bull. Korean Chem. Soc.* **2007**, *28*, 1573.
- (51) Albini, A.; Monti, S. *Chem. Soc. Rev.* **2003**, *32*, 238.
- (52) Lhiaubet-Vallet, V.; Cuquerella, M. C.; Castell, J. V.; Bosca, F.; Miranda, M. A. *J. Phys. Chem. B* **2007**, *111*, 7409.
- (53) Marians, K. J.; Hiasa, H. *J. Biol. Chem.* **1997**, *272*, 9401.
- (54) Lissi, E. A.; Encinas, M. V.; Lemp, E.; Rubio, M. A. *Chem. Rev.* **1993**, *93*, 699.
- (55) Llano, J.; Raber, J.; Eriksson, L. A. *J. Photochem. Photobiol., A* **2003**, *154*, 235.